
Article:
Wu, B., Li, J., Zhang, S. et al. (8 more authors) (2025) Study on the application amount optimization of water-based friction modifier based on field experiments. Proceedings of the Institution of Mechanical Engineers, Part F: Journal of Rail and Rapid Transit, 239 (2). pp. 96-105. ISSN 0954-4097

https://doi.org/10.1177/09544097241293578

Study on the application amount optimization of water-based friction modifier based on field experiments

Bingnan Wu[a], Jiaxin Li[a], Shuyue Zhang[a], Lubing Shi [a, b], Haohao Ding[a], Wenjian Wang[a, *], Zhongrong Zhou[a], Roger Lewis[c], Jianhua Zhou[d]

a. Tribology Research Institute, State Key Laboratory of Rail Transit Vehicle System, Southwest Jiaotong University, Chengdu 610031, China

b. Zhengzhou Research Institute of Mechanical Engineering Co., Ltd., Zhengzhou 450001, China

c. Department of Mechanical Engineering, The University of Sheffield, Mappin Street, Sheffield S1 3JD, UK

d. Central Research Institute (Qingshan), Baosteel Cooperation, Wuhan 430081, China

Abstract: The utilization of friction modifiers (FM) can reduce the adhesion coefficient of the top-of-rail to a moderate level, which could mitigate energy usage, damage propagation, noise and vibration at small radius curves. In this study, the influence of the FM application amount on the wheel-rail adhesion, noise and braking distance was explored under field conditions. Results showed that the FM application amount had a great influence on adhesion coefficient, noise and wheel-rail lateral force. When the FM application amount exceeded a threshold value, the braking distance of the locomotive was greatly extended and the adhesion control performance of FM reached saturation. The FM application amount and application frequency were finally optimized through a calculation process, which gave values of 0.33 mL/axle and 10 axles/application, respectively. These application parameters achieve the desired intermediate friction level along with an appropriate noise reduction and lateral force reduction.

Keywords: Railway transit; Wheel-rail adhesion; Friction modifier; Application amount

1 Introduction

In the domain of railway transit, many efforts have been put into research on wheel and rail protection for improving the safety and comfort of trains. The adhesion coefficient between the top-of-rail and the wheel tread is a vital parameter that helps control the level of the wheel-rail force[1]. A low adhesion coefficient can affect the traction and braking performance of trains and further jeopardize safety of trains. Sanding, applied from onboard trains directly into the wheel-rail interface can deal with most of the low adhesion cases. On the other hand, a high adhesion coefficient on the top-of-rail brings a series of problems, such as severe rolling contact fatigue (RCF) and rapid wear of wheel and rail materials, rail corrugation, and squealing[2, 3]. Gauge face oils and greases are not suitable for solving those problems as an extremely low adhesion coefficient would be produced if they were used which would have a negative effect on traction and braking. In high adhesion coefficient cases, where wear and RCF rates increase, grinding has been used and studied in attempts to prolong the lifespan of wheel and rail materials[4]. If the adhesion coefficient on the top-of-rail was adjusted to a moderate level, the material wear and noise could be alleviated and the low adhesion risk could be eliminated at the same time. This would reduce the need for multiple alternative solutions needed to deal with all the problems.

Products designed to control top-of-rail adhesion are described as friction modifiers (FMs). The Technology Transportation Centre Inc. (TTCI) in the US defines a FM as a product designed to provide an intermediate friction level over a range of material application rates and/or hold the friction constant over a specific range of wheel–rail creepage[5]. A number of different types exist[5] including drying, water based products and those based on oil or grease with a solid component.

The application process and carrydown mechanism of FMs are similar to that of gauge face grease[6]. Before curves, wayside application equipment pumps a certain amount of FM onto the top-of-rail according to the number of wheels passing[7]. When trains pass through the puddle of FM on the railhead, the FM adheres to the wheel tread and then it is carried down into the curves and

redeposited onto the rail. The adherent FM transfers back and forth between the wheel and rail surfaces until the FM is completely dried[8,9]. Trummer et al.[8] built a simulation model and argued that there were three mechanisms affecting carrydown for adherent FM, including pick-up, transfer, and consumption. Rahmani et al.[9] used a laser-induced fluorescence apparatus to detect the carrydown distance of FM and they found an interesting phenomenon that the FM adhering to the wheel-rail non-contact zone could re-enter the wheel-rail contact zone, which could result in a longer carrydown distance. After the FM is pumped onto the top-of-rail, the FM mixes with the wear debris from wheel and rail materials and then forms an FM third body layer with a certain shear strength[5]. It is the FM third body layer that brings a great deal of the desired effects, such as controlling adhesion coefficient, suppressing RCF development[10,11], alleviating squealing and noise[12,13], mitigating corrugation[14,15], and reducing energy consumption[5].

During the FM application process, an appropriate initial pumped amount is important since variations in the FM application amount can impact the carrydown distance of FM and lead to a transformation in lubrication regimes. This alteration directly determines the level of adhesion coefficient. In the wheel-rail interface, the FM third body layer and metal asperities of wheel and rail materials share the vertical force jointly, and the shear strength of FM third body layer is lower than that of metal asperities. In the case of a small FM application amount, the metal asperities bear more vertical force and thus produce a high adhesion coefficient[16,17]. In the case of a large FM application amount, the thickness of the FM third body layer is sufficient to flood the metal asperities, so the desired effects are achieved, such as longer carrydown distance[18] and less wear of wheel and rail materials[19]. However, the increase in the FM application amount is accompanied by a rapid decrease in the adhesion coefficient[20], which may cause the wheel to slip and endanger the safety of trains. Therefore, it is essential to apply FM in an appropriate amount for reaching an anticipated adhesion state.

The FM application amount depends on its material characteristics and application environment including different contact and temperature conditions. Galas et al.[18,19] used a ball-on-disc testing apparatus to compare different FM products and found that the performance of FM products was very different for the same application amount. This phenomenon could be attributed to the fact that the metal particles in FM products change the shear strength of the FM third body layers, so the tested FMs had different bearing capacities of vertical force. Wu et al.[17] prepared FMs with different solid particles and found that kaolin (solid particles) could give FM good friction control performance considering the wheel-rail adhesion and wear behavior. Kvarda et al.[21] found that when the FM application amount increased from 2 μL to 6 μL, the adhesion coefficients produced by some FMs stabilized at 0.25, and the adhesion coefficient produced by others were stabilized at an extremely low level (less than 0.05). Eadie et al.[22] pointed out that the specific FM application amount also depends on the curve radius, grades, traffic, train handling, and monitoring effectiveness, so it is a complex process with many variables. This makes it hard to determine the right amount of product to apply at the particular point on the track where it is needed. A wayside pump device implementation procedure has been proposed though based on a large number of long-term field tests. Li et al.[23] compared the FM adhesion control performance from 20 °C to -40 °C and found that the retentivity of FM increased yet the adhesion coefficient decreased with the decreasing temperature. Although the FM material characteristics and application conditions could influence the adhesion control performance of FM, an optimum amount for a specific application condition still exists. It is clear that there are many factors affecting FM performance and the wide range of products available makes it difficult to establish how much product should be applied for a particular usage scenario. More field testing, in particular, is needed to help make this decision.

In this study, a FM material was prepared and then tested at different application amounts using various field experimental approaches. A straight line and a curved line were used to carry out different tests. A hand-pushed tribometer was used to acquire the maximum available adhesion

coefficient (MAAC) under different conditions of top-of-rail surface. Image acquisition technology was used to determine the application frequency of FM. The equivalent film thicknesses were calculated according to the threshold values of FM application amounts. Finally, the FM optimum application amount and application frequency were calculated on the basis of a specific wayside application device.

2 Experimental methodology and details

2.1 Experimental material, equipment and line conditions

Five constituents were used to prepare the FM material[17]. The constituents were as follows: water, kaolin particles, graphite particles, acrylic resin emulsion, and sodium carboxymethyl cellulose (CMC). The quantities and functions of constituents are as shown in the Table 1. The steps for preparing the FM material were as follows: firstly, the required compositions were weighed out using an electronic balance. Secondly, the CMC was added to the water and the solution was stirred into a colloidal state using a blender with a mixing speed of 900 RPM. Thirdly, the kaolin, graphite particles, and acrylic resin emulsion were successively added into the colloidal solution. The stirring was continued until the solution was no longer changed. Fourthly, the suspension was hermetically sealed. After that, the FM material preparation was complete. The rotational viscosity of the prepared FM is 196.6 Pa·s.

Table 1 The quantities and functions of constituents

Constituent	Quantities (g)	Function
Water	96	Water is the carrier of all additives as the matrix material.
Kaolin particles	12	Kaolin particles are a type of mineral particles which are used to improve the COA level due to their high hardness.
Graphite particles	4	The lamellar graphite has a good lubricating function and thermal stability, and is a common lubrication solid particle in water-based lubricants
Acrylic resin emulsion	16	The acrylic polymer emulsion is selected as the binder and acts to increase the binding ability of the FM.
Sodium carboxymethyl	3	The polymer chains of CMC entangle in the water-based material and prevent the solid particles or acrylic resin

cellulose (CMC) polymers from polymerizing and sinking in the solution.

Fig. 1 shows the experimental apparatus and line conditions. The hand-pushed tribometer is shown in Fig. 1a. This device is pushed forward along the track. As the tribometer progresses, an increasing vertical force is applied on the testing rollers until a slip event happens. At the moment of sliding at the contact point, the tangential force is collected by the device, and then it is divided by the vertical force to obtain the adhesion coefficient, which is the MAAC[24]. The hand-pushed tribometer was pushed at a normal walking speed (about 1 m/s), and the MAAC was read from the screen of the integrated box approximately every 2 to 3 m.

(a)

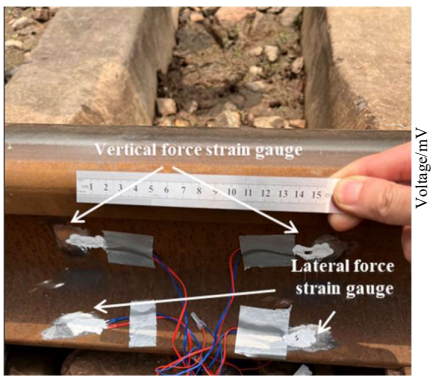

(b)

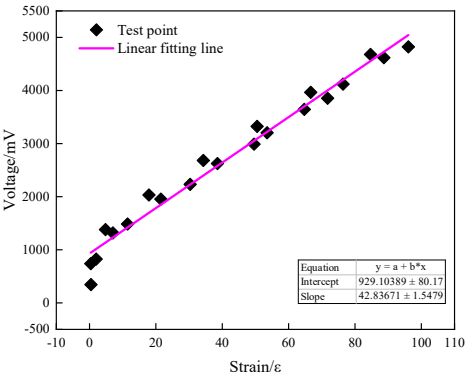

(c)

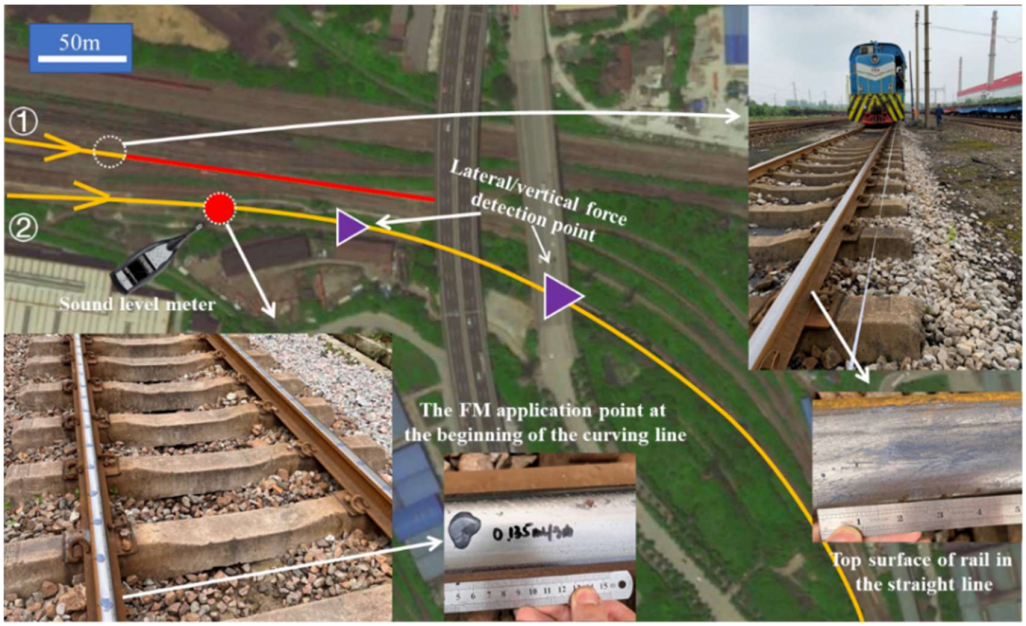

(d)

Fig. 1 The experimental apparatus and line conditions: (a) the hand-pushed tribometer; (b) lateral/vertical force strain gauge set-up; (c) calibrated curve of strain-voltage; (d) schematic of the field lines and images of the rail surface after applying FM

A series of strain gauges (Fig. 1b) were used to measure the magnitude of wheel-rail force, including lateral force and vertical force. Before testing, a de-rusting process was performed and then the strain gauges were stuck onto the rails. The lateral force strain gauge was stuck onto the top of the rail foot and the vertical force gauge was stuck onto the middle of the rail web. Then, a full bridge circuit based on the shear stress detection method was constructed[25]. After that, a coefficient of proportionality between the voltage obtained using the signal acquisition system and the force produced by a portable hydraulic loading system was determined (Fig. 1c). When trains passed through the position with strain gauges, the wheel-rail force made the full bridge circuit produce a voltage, which can be converted into wheel-rail force during data processing using the determined coefficient.

A sound level meter (Brüel & Kjær 2250, Denmark) was used to measure the wheel-rail noise and ambient noise in the curved line tests. The sound meter was held 5m from the center of the track, with the microphone 1.2m above the height of the rail. The equivalent continuous A-weighted sound pressure level (LAeq, dB) is ten times the logarithm base 10 of the ratio between the average square sound pressure P_A squared and the reference sound pressure P_0 (2×10^{-5}) squared within a certain period of time (Eq. (1), T=0.5s). The experiment measured the maximum LAeq when each train passed through the FM application point. A Fourier transform was performed on the time-domain data, resulting in a frequency spectrum plot of the sound pressure levels from the moment the train enters the FM application point until it leaves. Following this, a weighting based on the sensitivity of the human ear to different frequencies was applied to the sound pressure level spectrum using the specific sound processing software, resulting in a weighted sound pressure (dBA) spectrum.

$$L_{Aeq} = 10lg\frac{\frac{1}{T}\int_{t_1}^{t_2} p_A^2(t)dt}{p_0^2} \quad (1)$$

Fig. 1d shows a schematic of the field straight line and curved line and images of the top-of-rail after applying the FM. Both lines are in-service at a steel factory. The length of the straight line is about 1 km. A GK1B diesel locomotive with an axle load of 23t was employed to perform braking tests on the straight line. This locomotive is equipped with disc brakes. The curved line is used to transport goods into the factory. The radius, length, and superelevation of the curved line are 500 m, 529 m, and 35 mm, respectively. The main locomotives and vehicles running on the curved line are GK1B, C70, and C64. C70 and C64 are two different types of freight wagons. The train arrangement is about forty wagons pulled by one locomotive. The speed of the train on the curved line is about 20 km/h and the average axle load is about 23 t.

2.2 Experimental methodology

Table 2 shows the FM application amounts and measured parameters for the straight line and curved line. The temperature and humidity during field testing were 25~30℃ and 57~63%, respectively.

Table 2 FM application amounts in the straight line and curved line

Test apparatus and line condition	Straight line		Curved line		
	The maximum available adhesion coefficient	Braking distance	The maximum available adhesion coefficient	Noise	Wheel-rail force
FM application amounts	0		0	0	
	0.135 mL/m		-	0.135 mL/axle	
	0.3 mL/m		-	0.3 mL/axle	
	0.5 mL/m		0.5 mL/axle	0.5 mL/axle	
	0.75 mL/m		-	0.75 mL/axle	
	1 mL/m		-	1 mL/axle	
	3 mL/m		-	-	

On the straight line, the MAAC tests and braking tests were carried out. In the MAAC tests, a quantity of FM was applied to the top-of-rail for each meter on the right rail using the manual dispenser. Then the FM was smoothed into a wet film using a brush, and a dried FM third body layer was obtained after waiting for an hour (Fig 1d). The MAAC of the film in wet and dry conditions on the right rail was tested via the hand-pushed tribometer. In the braking tests, the FM film was produced on the top-of-both rails using the manual dispenser and a brush. The length of the FM film applied to the rails was 50 m because the maximum braking distance generated by the oil-based friction modifier is 50 m[26]. The average velocity of the locomotive had reached 24 km/h before arriving at the FM applied area. The locomotive began to brake when its first braking axle reached the FM application area, and the braking pressure of the braking shoes was about 2.2 bar/cm^2. When the train was stopped, the distance between the point where the locomotive started braking and the stationary point was measured and defined as braking distance. After each brake test, wheel surfaces were cleaned with damp clothes until the FM was no longer visible before conducting the next test.

On the curved line, a total application amount was calculated according to the FM application amount to be tested in Table 2 and the number of passing wheelsets. Then this total application amount was divided equally into fifteen smaller amounts. After that, the FM was applied in a small amount onto the top surface of two rails every 20 cm over 3 m, which was about the circumference of the wheel (Fig. 1d). The above FM application operation was performed approximately three minutes before the train passed. The MAACs were measured using the hand-pushed tribometer under dry, light rain, and FM conditions. The noise at the FM application point was measured with the sound level meter. The wheel-rail forces at the FM application point and the curve middle point were measured by the wheel-rail force measurement system. The derailment coefficient and the rate of wheel load reduction were calculated using the collected wheel-rail forces to evaluate the train safety. The derailment coefficient was used to assess the risk of the wheel climb and train derailment. Eq. (2) was used to calculate the coefficient of derailment. Q is the wheel-rail lateral force and P was

the vertical force. The rate of wheel load reduction was used to evaluate the derailment possibility caused by excessive wheel load reduction. Eq. (3) was used to calculate the rate of wheel load reduction, where P_1 is the reduced wheel load, and P_2 is the increased wheel load.

$$Coefficient\ of\ derailment = \frac{Q}{P} \tag{2}$$

$$Rate\ of\ wheel\ load\ reduction = \frac{P_2 - P_1}{P_2 + P_1} \tag{3}$$

3 Results

3.1 MAACs and braking distances in the straight line

The MAACs obtained in the and field using the hand-push tribometer are shown in Fig. 2a. The MAAC of clean rail surface is 0.52. An increase in the FM application amount leads to a decrease in the MAAC in both dry and wet FM conditions. The adhesion coefficient of dry and wet FM is about 0.4 and 0.37, respectively, for the application amount of 0.135 mL/m. When the FM application amount reaches 0.3 mL/m, the adhesion coefficients reduce to 0.12 and 0.17 under wet and dry FM conditions, respectively. Based on Chinese testing standards[27,28], the surface roughness *Ra* of top-of-rail surface in the field was measured using a roughness tester (JB-6C, China), and the test results are shown in Fig. 2b. The surface roughness Ra of field top-of-rail surface was 14.64 μm. In the literature[9], it was found that the thickness of the FM film at a curve does not exceed 15μm, which almost coincides with the numerical value of the surface roughness of the steel rail. This implies that the normal load is borne jointly by the FM film and the metal asperities and the wheel-rail interface is in a mixed lubrication regime. Increasing the application amount will reduce the normal load on the metal asperities and decrease the adhesion coefficient. According to the high roughness of rail surface, there is a high combined roughness of wheel and rail thus the normal load is borne jointly by the FM film and the metal asperities and the wheel-rail interface is in a mixed lubrication regime. Increasing the application amount will reduce the normal load on the metal asperities and decrease the adhesion coefficient.

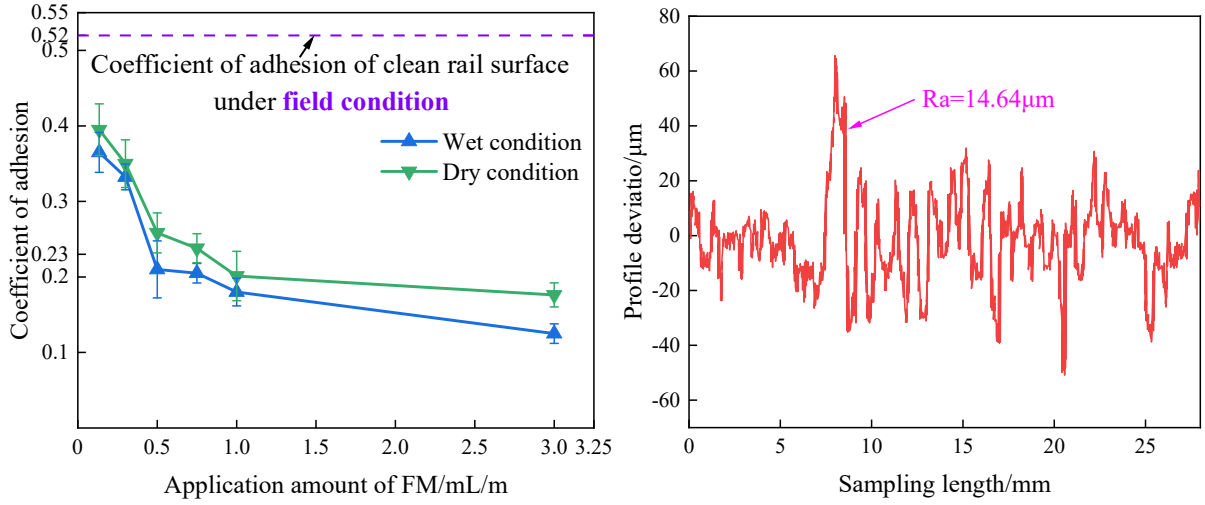

(a) (b)

Fig. 2 (a)The maximum available adhesion coefficients (MAAC) in the straight line and (b) surface roughness *Ra* of top-of-rail

The results of braking tests on the straight line are shown in Fig. 3. Under the clean condition, the braking distance of the locomotive is about 20.4 m. The results show that the braking distance was not affected by the FM when the application amount was less than 0.5 mL/m. This application amount can provide a moderate adhesion coefficient level and lubrication regime for the wheel-rail interface. A noticeable growth of braking distance occurred when the FM application amount exceeded 0.5 mL/m. The braking distance increases from 25.3 m to 44.3 m when the FM application amount increases from 0.75 mL/m to 3 mL/m. Fig. 4 shows the images of the rail surfaces after four braking tests. The width of the FM removal zone reduces and the amount of the residual FM third body layer increases with an increase in the FM application amount. It is difficult for the wheel-rail force to completely remove the FM third body layer with excessive thickness for large FM application amounts. From the braking test, it was found that the threshold value of FM application amount is 0.5 mL/m.

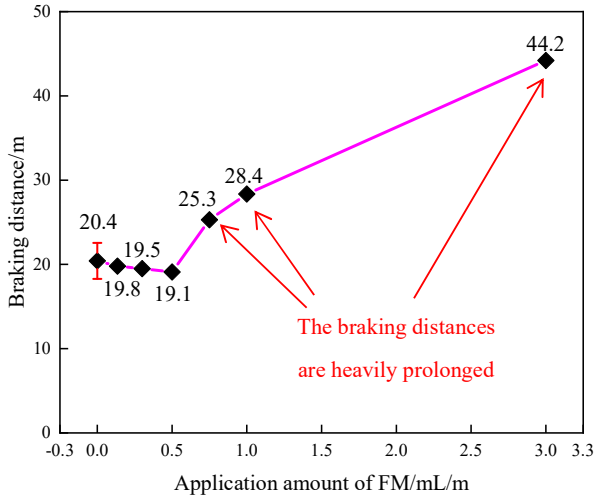

Fig. 3 The braking distance at different FM application amounts

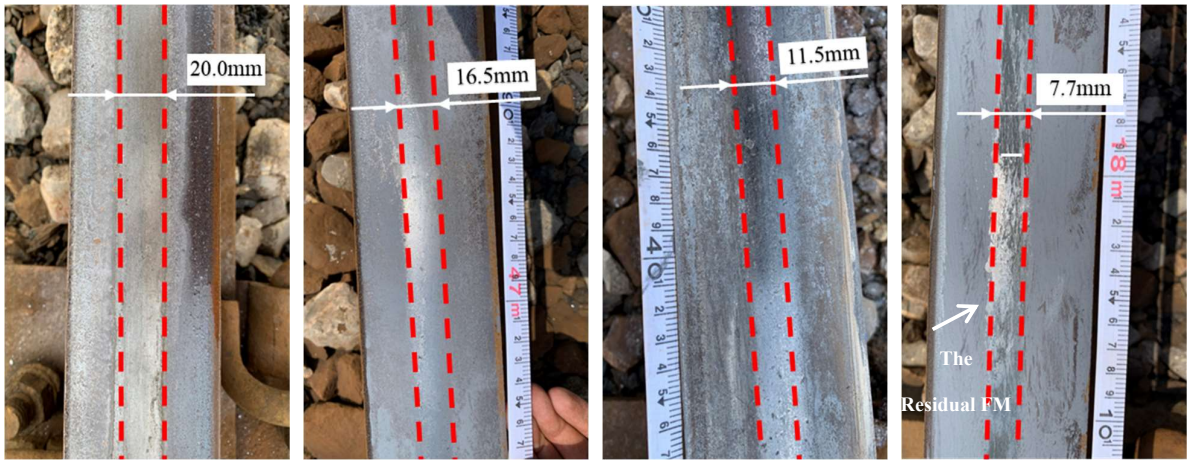

(a) (b) (c) (d)

Fig. 4 The surfaces of top-of-rail after braking tests: (a) 0.135 mL/m; (b) 0.75 mL/m; (c) 1 mL/m; (d) 3 mL/m.

3.2 Noise, MAACs, and wheel-rail force in the curved line

The noise test results are shown in Fig. 5. The wheel-rail noise at the FM application point is alleviated after applying the FM. The FM application amount has a significant influence on the effect of noise mitigation. The basic noise level is the LAeq when there is without trains pass through the FM application position. When the application amount of FM increases from 0.135 mL/axle to 0.3 mL/axle (Fig. 5a), the average sound decreases from 85.1 dB to 79.8 dB. Regarding the noise spectrum, noise within the range of 30-5,000Hz is categorized as rolling noise at the top-of-rail (with

noise between 1,000-5000Hz being identified as top-of-rail squeal), while noise frequencies exceeding 5,000Hz are classified as wheel flange squeal[29]. As shown in Fig. 5b, after the application of FM, there is a reduction in high-frequency squeal at the wheel flanges and rolling noise at the top-of-rail. This result is consistent with the example of a tram system in Japan[29], where the noise reduction effect was more pronounced when FM was applied to both rails.

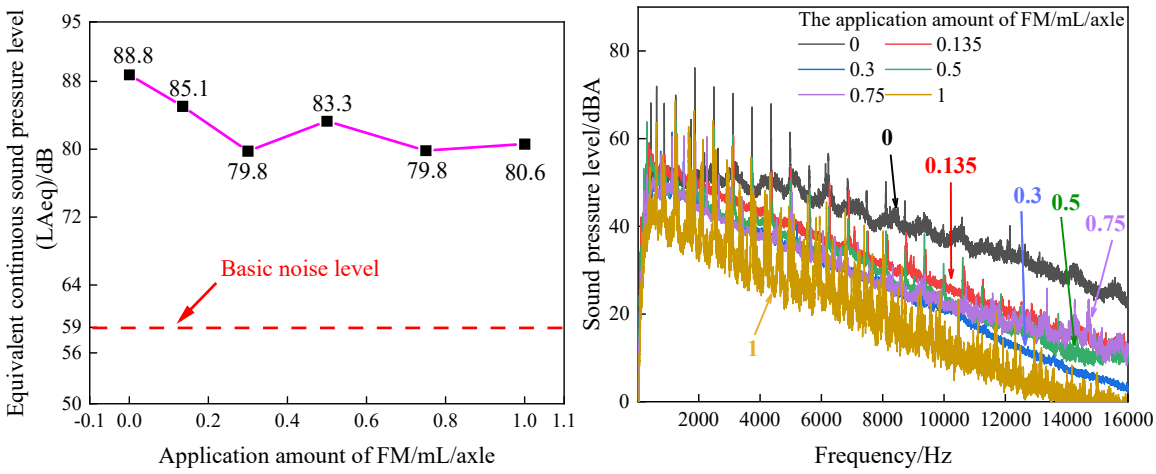

(a) (b)

Fig. 5 Noise in the curved line: (a) equivalent continuous sound pressure level; (b) sound pressure level spectrum.

Fig. 6 shows the MAAC obtained for the curved line. For both outer and inner rails, results can be divided into Area I and Area II according to the adhesion coefficient level under FM conditions. Area I can be considered as the effective adhesion control region of FM, while Area II can be regarded as the semi-failure region of FM. The demarcation points of Area I and Area II from the FM application point on the outer rail and inner rail are about 100 m and 60 m, respectively. For the outer rail, the order of the MAACs in all states from high to low is dry, light rain, and FM in Area I. In Area II, the MAAC for FM is slightly lower than that of the dry state. The MAAC for light rain is the lowest. The difference between the inner rail and outer rail is that in Area II under FM condition, the MAAC is slightly higher than in the dry state for the inner rail. The possible reason for this may be because more FM is consumed on the inner rail as the train navigates the curve (detailed reasons will be analyzed in the last paragraph of this section), resulting in a shorter distance for Area I on the

inner rail. Accordingly, the MAAC measured under FM conditions can be approximately considered as the MAAC under dry conditions.

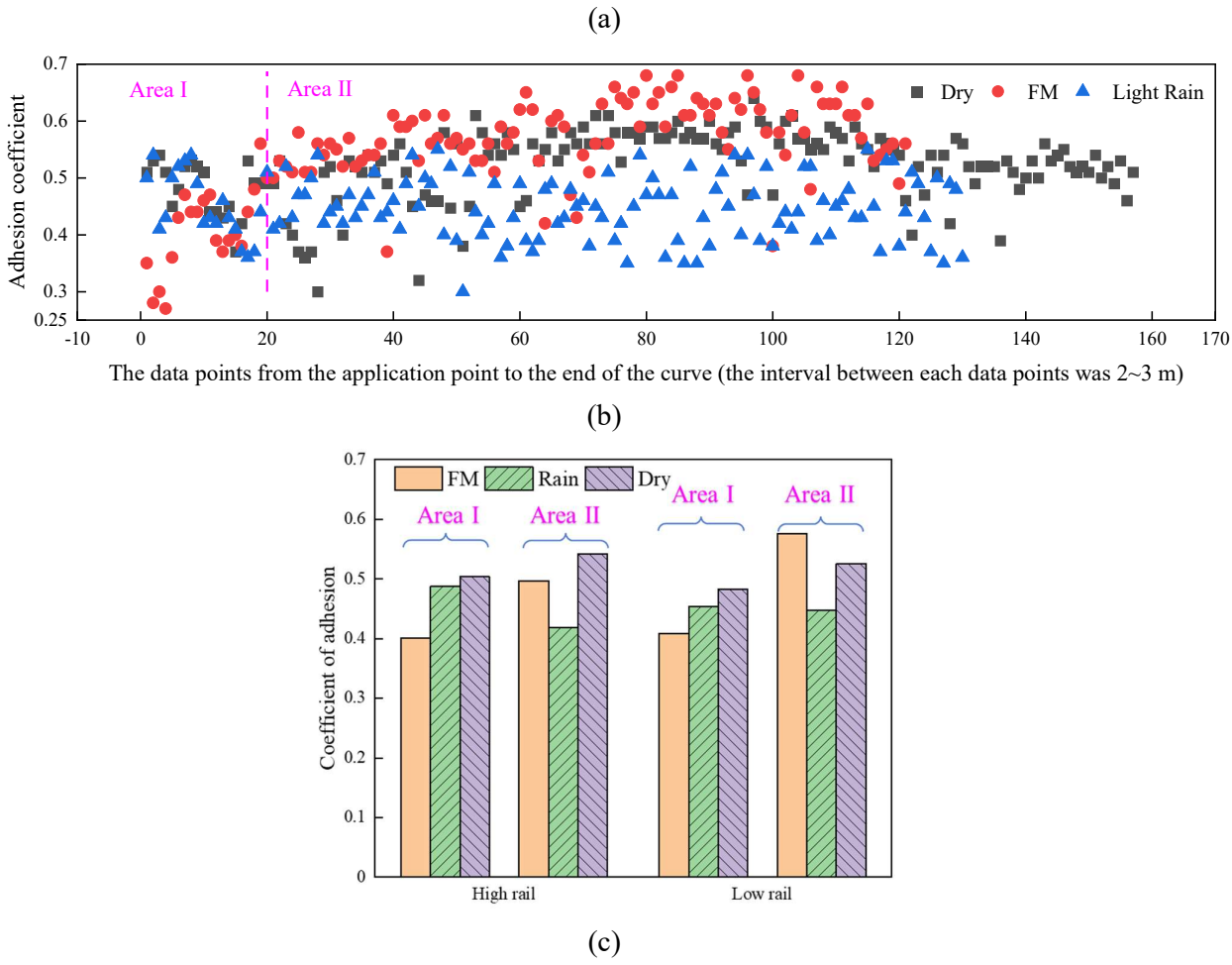

Fig. 6 The maximum available adhesion coefficient of the top-of-rail under dry, light rain, and FM conditions: (a) outer rail; (b) inner rail; (c) average coefficient of adhesion in Area Ⅰ and Area Ⅱ

The results of wheel-rail forces are shown in Fig. 7. The plotted data was the maximum value of wheel-rail force within the first ten wheels pass. The most noticeable variation is the lateral force on

the inner rail at the FM application point. As the FM application amount increases, the lateral force on the inner rail first decreases and then stabilizes. The FM application amount at which the reduction in lateral force reaches saturation is 0.3 mL/axle. The excellent lateral force control on the inner rail by FM is consistent with the results presented in[30, 31]. The decreased lateral force is helpful for the protection of rail fastenings and ballast and alleviation of noise and vibration. From the Fig. 7, the vertical force on the inner rail is higher than that on the outer rail at the FM application point. When the train reaches the middle of the curve, the lateral movement decreases, and the vertical forces on the inner and outer rails tend to be the same. Fig. 8 shows the derailment coefficient and wheel load reduction rate of the train at the FM application point. The derailment coefficient of the train needs to be less than 0.8, and the wheel load reduction rate needs to be less than 65%[25]. Although the train has already stayed within the safety limits for these two values when passing through this curve, the application of FM can still reduce the derailment coefficient and wheel load reduction rate on the inner rail.

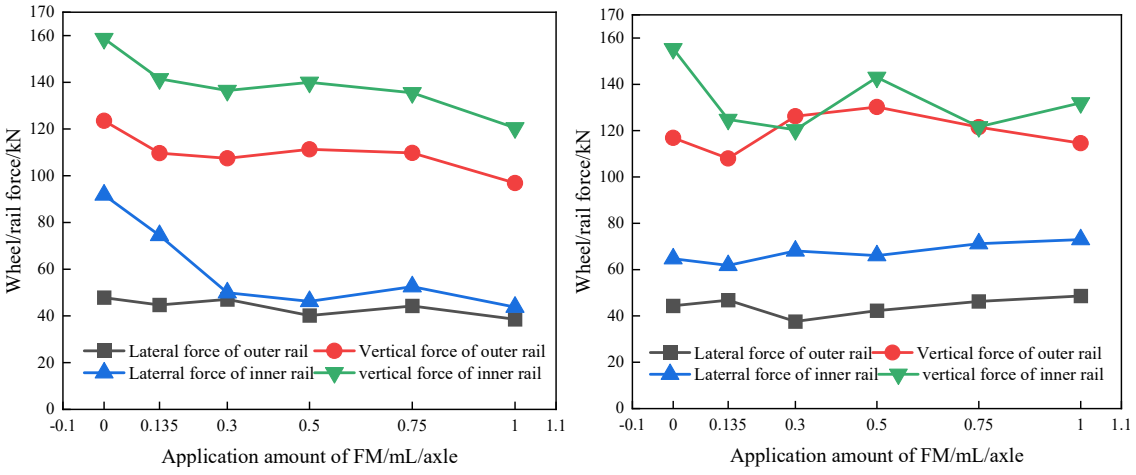

Fig. 7 The wheel-rail force of the curved line: (a) the FM application point; (b) the center point

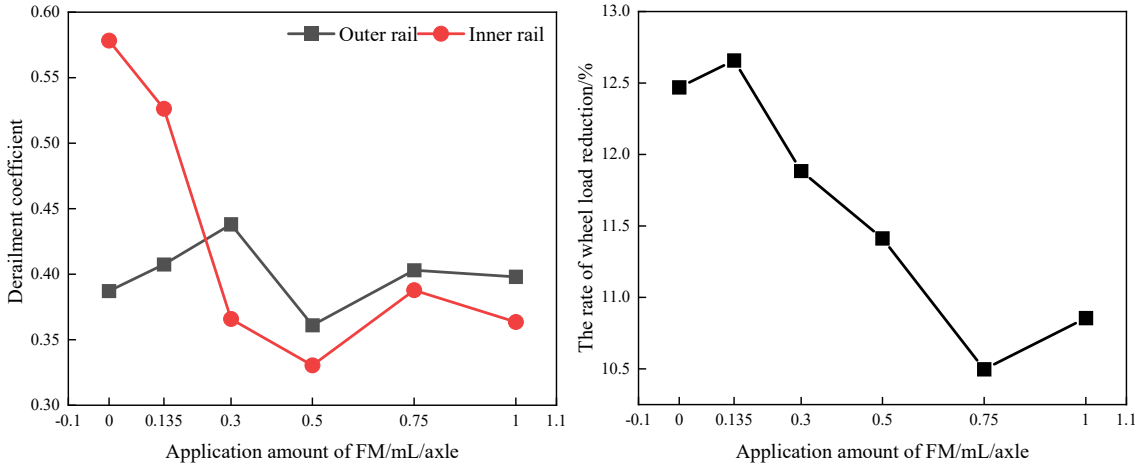

(c) (d)

Fig. 8 The safety analysis of the curved line (a) derailment coefficient; (b) wheel load reduction rate.

Under dry conditions, as the train arrives at a curve, the wheelsets experience lateral movement, causing the wheel diameter in contact with the inner rail to be greater than that in contact with the outer rail. When the driving torque is applied to the wheelsets, the wheel tread contacting with the inner rail generates a driving force higher than that on the wheel tread contacting with the outer rail, resulting in a torque that is in the opposite direction to the curve on the entire train[31]. Under the influence of this torque, the outer wheel flange tends to experience severe sliding friction, leading to significant wear and noise. With the application of FM, the adhesion coefficient on both the inner and outer rails is reduced (Fig. 6), leading to a decrease in longitudinal wheel-rail force and a weakening of the torque in the opposite direction of the curve. Then the tendency for lateral movement of wheels can be mitigated, reducing the friction of wheel flange and subsequently lowering wheel flange squeal (Fig. 5), derailment coefficient, and wheel load reduction rate (Fig. 8). It worth noting that the higher wheel-rail forces (Fig. 7) contribute to the more FM consumption[32] and this is why the distance in Area I on the inner rail is shorter (Fig. 6).

3.3 The application frequency and application amount of FM

The field tests indicated that there is a threshold value of FM application amount, for which noise and lateral force reduction occurs, train safety improves, and there is no significant effect on

braking performance of the train. The increase in the FM application amount could prolong the retentivity and boost the FM performance in the curved line. However, when the FM application amount exceeded the threshold value, a low adhesion state was produced, and the braking distance of the locomotive was extended. In this section, high-frame-rate image and distribution images from phone camera were used to determine the application frequency. Furthermore, the film thicknesses corresponding to the threshold value in each test were calculated by a simplified model. Finally, an optimized FM application amount and application frequency were put forward.

Fig. 9 shows movements and distributions of FM for the curved line. The FM flow movements in the curved line were mainly through adherence to the wheel and squeeze-out from the wheel-rail interface (Fig. 9a). As can be seen in Fig. 9b and c, some FM was squeezed out and some FM was carried into the curved line by the adhering movement. As the number of wheels passing through the FM application point increased, the FM adhering and squeeze-out movements diminished. The FM movements could not be observed at the FM application point after the passing of ten wheels. Accordingly, the FM adhering movement stopped after the passing through of about ten wheels, which means that the FM should be re-pumped onto the top-of-rail within ten wheel passes. Manually increasing the FM application amount mainly increased the FM amount adhered to the wheels. However, the growth of FM carrydown amounts in the adhering movement was finite because there was no one continuous and stable supply for FM in this study.

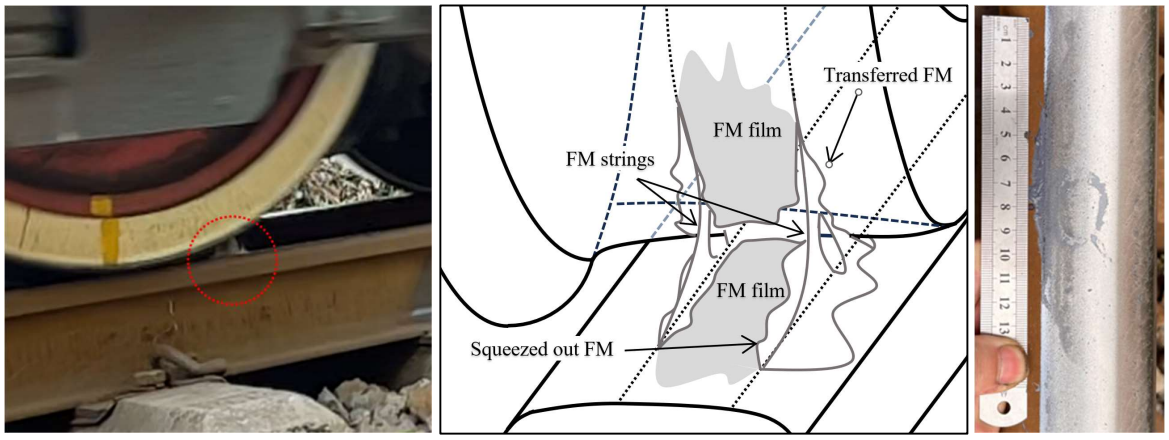

(a) (b) (c)

(d) (e) (f) (g) (h)

Fig. 9 The movements and distributions of FM in the curved line: (a) the 1st wheel passing the FM puddle; (b) FM distributions during the 1st wheel-rail interaction; (c) residual FM at the application point; (d) residual FM in the curved line; (e) FM returned to rail surface; (f) accumulated FM; (g) FM in the RCF cracks; (h) wasted FM;

Furthermore, Fig. 9d to h show the FM distributions on the surface of the rail in the curved line. The typical FM distributions on the rail surface in the curved line include: (1) residual FM in the center of the wheel-rail contact zone (Fig. 9d); (2) FM returned to the rail surface (Fig. 9e) and accumulated FM third body layer (Fig. 9f), which was produced by wheel transverse movement; (3) FM in RCF cracks; (4) wasted FM. The wasted FM comes from the FM adhered to the wheels with some of it being flung off during rapid wheel rotation and subsequently going to waste. The increase in the FM application amount could simultaneously increase the amount of the above four FM distributions. Correct application of FM can alleviate RCF crack growth, i.e. application before cracks are initiated. Application, after crack initiation can, however, accelerate RCF crack development due to the hydraulic crack growth mechanism and possibility of lower crack face friction. Using a water-based rather oil-based top-of-rail product reduces this risk though[10].

The calculation of application amount of FM was achieved through a simplified model, in which the key parameters are the equivalent film thickness obtained through field tests and the shape of FM

pumped from the pump plate. Fig. 10 shows the calculation process and schematics of FM application amount and application frequency. Firstly, two threshold values of FM application amounts were calculated and the results are shown in Table 3. The theoretical thicknesses of FM third body layers in the straight line and curved line tests were 10 μm and 2.1 μm, respectively. The former is a threshold value for safety, while the latter is a threshold value for performance saturation. Therefore, the average value of 10 μm and 2.1 μm was taken as the desired film thickness of the FM third body layer, which is 6.05 μm. The assumed contact size of wheel-rail contact zone, whose width and length were assumed as both 15 mm, was attempted to multiply with this calculated film thickness, which was 1.36×10^{-3} mL. This value represents the ideal film thickness of FM third body layer when the train passes through the FM application point.

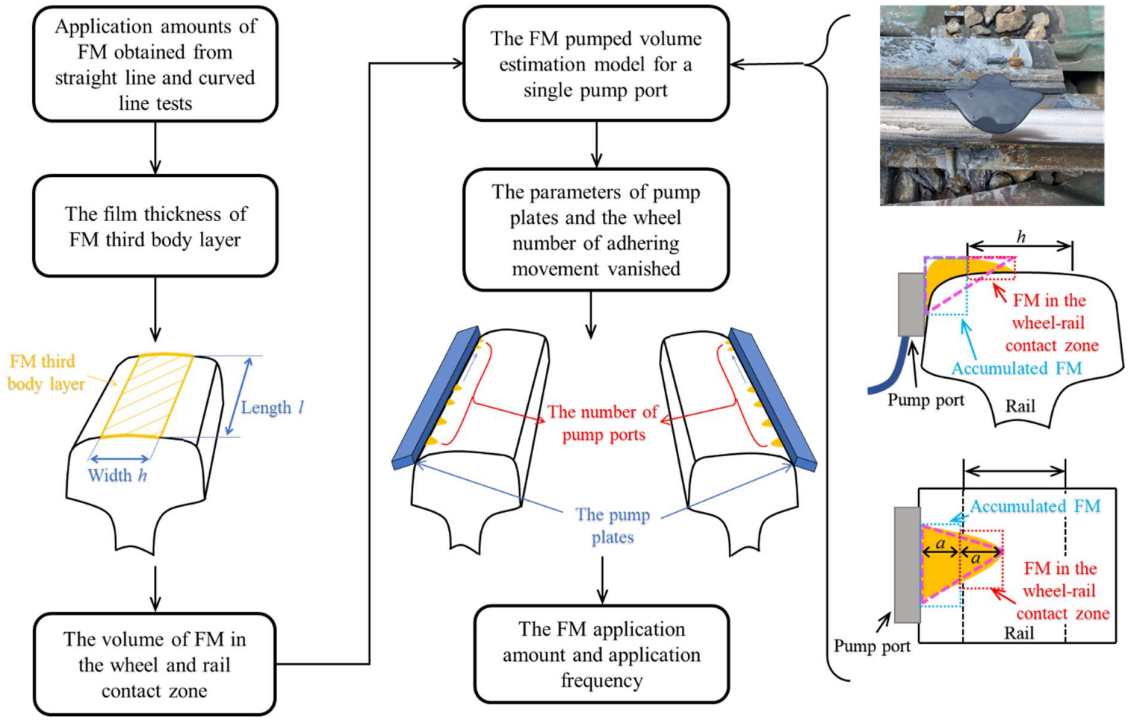

Fig. 10 The calculation process and schematics of FM application amount and application frequency: (a) shape of FM after its application under field condition; (b) the thickness of FM third body layer; (c) calculation process; (d) the front view and (e) the top view of the FM pumped volume estimation model; (f) the pump plates.

Table 3 The calculation parameters and results of FM film thickness

Test site	Test items	FM critical application amount *A*	Contact form	Width of FM third body layers (*h*)	Length of FM third body layers (*l*)	Theoretical critical FM film thickness calculation formula	FM film thickness
Straight line	Braking distance	0.5 mL/m	Surface	50 mm	1000 mm	$A/(h*l)$	10 μm
Curved line	Noise and wheel-rail force	0.3 mL/axle	Surface	50 mm	π*910 mm (diameter of wheel)		2.1 μm

The FM shape, after its application in field conditions, can be regarded as being approximately a triangular pyramid based on the rail profile and can be divided into two parts including accumulated FM and FM in the wheel and rail contact zone. Hence, it is possible to estimate the application volume of FM for individual pump ports by utilizing the volume of FM in the wheel and rail contact zone, which was 1.36×10^{-3} mL. The volume of FM in the wheel-rail contact zone (calculated above) is one-eighth of the FM pump volume of a single pump port, which can be calculated as 1.09×10^{-2} mL. Furthermore, the pump equipment is assumed to have one pump plate on each of the left and right rails with 15 pump ports in each pump plate. The application amount of FM for the given pump equipment is the value obtained by multiplying the FM pump volume of a single pump port and the number of pump ports on the pump plates (that was 30). As a result, the FM application amount for the given pump equipment can be calculated to be approximately 0.33 mL/axle. It is important to note that this value mainly consists of accumulated FM to ensure its carrydown mechanism. The actual value should be slightly higher than this figure to enhance the carrydown capacity of FM.

The optimized application frequency and FM application amount is 0.33 mL/axle and 10 axles/time, respectively. These application parameters achieve the desired intermediate friction level along with an appropriate noise reduction and lateral force reduction. It should be noted that these

results are based on a specific line and an assumed pump equipment, and the actual FM application amount and application frequency need to be adjusted according to the specific conditions.

5. Conclusions

This study evaluated the effect of different FM application amounts on FM adhesion control performance in straight line and curved line. The threshold values of FM application amounts were obtained. Then a calculation process was developed to calculate the FM application amount. Finally, the optimized FM application amount and application frequency were obtained. The main conclusions are as follows:

(1) In the straight line, the braking distance is not affected by the FM when the application amount is less than 0.5 mL/m. In the curving line, the FM application amount of 0.3 mL/axle could achieve saturation adhesion control performance.

(2) When the application amount of FM increases from 0.135 mL/axle to 0.3 mL/axle, the average sound decreases from 85.1 dB to 79.8 dB. There is a reduction in high-frequency squeal at the wheel flanges and rolling noise at the top-of-rail.

(3) In the straight line, an increase in the thickness of FM third body layer prolonged the braking distance of the train. In the curved line, an increase in the FM application amount mainly raised the FM amount in the adhering movement, which resulted in an increase in the FM amount on the rail surface in the curved line.

(4) The calculation results of the thickness of FM third body layer showed that the critical thickness in the straight line and curved line tests were 10 μm and 2.1 μm, respectively. The thickness could be converted into an FM application amount based on the given pump equipment and the simulation process developed in this study. For the FM used in this study, the optimized FM application amount and application frequency were 0.33 mL/axle and 10 axles/time. These application parameters achieve the desired intermediate friction level along with an appropriate noise reduction and lateral force reduction.

Acknowledgements

The work was supported by National Natural Science Foundation of China (Nos. 52272443, 52027807), Natural Science Foundation of Sichuan Province (No. 2022NSFSC0036) and Fundamental Research Funds for the Central Universities (No. 2682023ZTPY022).

Declaration of competing interest

The authors have no competing interests to declare that are relevant to the content of this article.

References

[1] Zhang SY, Spiryagin M, Ding HH, et al. Rail rolling contact fatigue formation and evolution with surface defects. *International Journal of Fatigue* 2022; 158: 106762.

[2] Hu Y, Zhou L, Ding HH, et al. Microstructure evolution of railway pearlitic wheel steels under rolling-sliding contact loading. *Tribology International* 2020; 154: 106685.

[3] Liu S, Silva UD, Chen D, et al. Investigation of wheel squeal noise under mode coupling using two-disk testrig experiments. *Wear* 2023; 530-531: 205035.

[4] Ding H, Yang J, Wang W, et al. Characterization and formation mechanisms of rail chips from facing grinding by abrasive wheel. *Journal of Manufacturing Processes* 2022; 73: 544-554.

[5] Stock R, Stanlake L, Hardwick C, et al. Material concepts for top of rail friction management-Classification, characterisation and application, *Wear* 2016; 366–367: 225-232.

[6] Harmon M, Powell B, Barlebo-Larsen I, et al, Development of Grease Tackiness Test. *Tribology Transactions* 2019; 62(2): 207-217.

[7] Khan SA, Lundberg J, Stenström C. Carry distance of top-of-rail friction modifiers. *Proceedings of the Institute of Mechanical Engineers, Part F: Journal of Rail and Rapid Transit* 2018; 232(10):2418-2430.

[8] Trummer G, Lee ZS, Lewis R, et al. Modelling of Frictional Conditions in the Wheel-Rail Interface Due to Application of Top-of-Rail Products, *Lubricants* 2021; 9(10): 100.

[9] Rahmani H, Gutsulyak D, Stanlake L, et al. Carrydown of liquid friction modifier. *Proceedings of the Institute of Mechanical Engineers, Part F: Journal of Rail and Rapid Transit* 2022; 236(9): 1124-1134.

[10] Hardwick C, Lewis R, Stock R, The effects of friction management materials on rail with pre-existing rcf surface damage. *Wear* 2017; 384-385: 50-60.

[11] Song J, Shi L, Ding H, et al. Effects of solid friction modifier on friction and rolling contact fatigue damage of wheel-rail surfaces. *Friction* 2022; 10(4): 597-607.

[12] Meehan PA, Liu X. Modelling and mitigation of wheel squeal noise under friction modifiers. *Journal of Sound and Vibration* 2018; 440: 147-160.

[13] Liu X, Meehan PA. Investigation of squeal noise under positive friction characteristics condition provided by friction modifiers. *Journal of Sound and Vibration* 2016; 371: 393-405.

[14] Eadie DT, Santoro M, Oldknow K, et al. Field studies of the effect of friction modifiers on short pitch corrugation generation in curves. *Wear* 2008; 265: 1212-1221.

[15] Eadie DT, Santoro M. Top-of-rail friction control for curve noise mitigation and corrugation rate reduction. *Journal of Sound and Vibration* 2006*;* 293: 747-757.

[16] Li Q, Shi L, Zhang S, et al. Recovery Process of wheel/rail adheison under the action of water-based friction modifier. China Surface Engineering 2022; 35:107-111.

[17] Wu B, Shi L, Ding H, et al. Influence of different solid particles in friction modifier on wheel-rail adhesion and damage behaviours. *Wear* 2023; 522:204833.

[18] Galas R, Kvarda D, Omasta M, et al. The role of constituents contained in water–based friction modifiers for top–of–rail application, *Tribology International* 2018; 117: 87-97.

[19] Galas R, Omasta M, Krupka I, et al. Laboratory investigation of ability of oil-based friction modifiers to control adhesion at wheel-rail interface. *Wear* 2016; 368-369: 230-238.

[20] Li Q, Wu B, Ding H, R. et al. Numerical prediction on the effect of friction modifiers on adhesion behaviours in the wheel-rail starved EHL contact. *Tribology International* 2022; 170: 107519.

[21] Kvarda D, Skurka S, Galas R, et al. The effect of top of rail lubricant composition on adhesion and rheological behaviour. *Engineering Science and Technology, an International Journal* 2021; 35: 101100.

[22] Eadie DT, Oldknow KD, Maglalang L, et al. Implementation of wayside top of rail friction control on North American heavy haul freight railways. In: Proceedings of the World Congress on Railway Research(WCRR 2006), Quebec, Canada, 4-8 June 2006.

[23] Li JX, Wu BN, Ding HH, et al. Wear and damage behaviours of wheel and rail materials: Effects of friction modifier and environmental temperature. *Wear* 2023; 523: 204796.

[24] Harmon M, Santa J, Jaramillo J, et al. Evaluation of the coefficient of friction of rail in the field and laboratory using several devices. *Tribology-Materials, Surfaces & Interfaces* 2020; 14: 119-129.

[25] Tang J, Luo Y, Liao B, et al. Research on wheel-rail force derailment coefficient and wheel load reduction ratio of the scientific research track line. *Journal of Hebei University of Engineering (Natural Science Edition)* 2017; 4 (34): 51-56.

[26] Galas R, Omasta M, Klapka M, et al. Case Study: the Influence of Oil-based Friction Modifier Quantity on Tram Braking Distance and Noise. *Tribology in Industry* 2017; 39: 198-206.

[27] CN-GB. GB/T 1013-2009 Geometrical product specifications (GPS) - Surface texture: Profile method - Surface roughness parameters and their values. GB, 2009.

[28] CN-GB. GB/T 33523.1-2020 Geometrical product specifications (GPS)—Surface texture: Areal—Part 1: Indication of surface texture. GB, 2020.

[29] Eadie DT, Santoro M, Kalousek J. Railway noise and the effect of top of rail liquid friction modifiers: Changes in sound and vibration spectral distributions in curves. *Wear* 2005; 258: 1148-1155.

[30] Chen H, Fukagai S, Sone Y.et al. Assessment of lubricant applied to wheel/rail in curves. *Wear* 2014; 314: 228-235.

[31] Matsumoto A, Sato Y, Ohno H, et al. Improvement of bogie curving performance by using friction modifier to rail/wheel interface Verification by full-scale rolling stand test. *Wear* 2005; 258: 1201-1208.

[32] Wang W, Li S, Ding H, et al. Wheel/rail adhesion and damage under different contact conditions and application parameters of friction modifier. Wear 2023; 523: 204870.